

MINIMUM BOUNDING POLYTROPES FOR ESTIMATION OF MAX-LINEAR BAYESIAN NETWORKS

KAMILLO FERRY

ABSTRACT. Max-linear Bayesian networks are recursive max-linear structural equation models represented by an edge weighted directed acyclic graph (DAG). The identifiability and estimation of max-linear Bayesian networks is an intricate issue as Gissibl, Klüppelberg, and Lauritzen have shown. As such, a max-linear Bayesian network is generally unidentifiable and standard likelihood theory cannot be applied.

We can associate tropical polyhedra to max-linear Bayesian networks. Using this, we investigate the minimum-ratio estimator proposed by Gissibl, Klüppelberg, and Lauritzen and give insight on the structure of minimal best-case samples for parameter recovery which we describe in terms of set covers of certain triangulations.

We also combine previous work on estimating max-linear models from Tran, Buck, and Klüppelberg to apply our geometric approach to the structural inference of max-linear models. This is tested extensively on simulated data and on real world data set, the NHANES report for 2015–2016 and the upper Danube network data.

1. INTRODUCTION

Graphical models are a powerful tool for modeling the dependencies of multivariate random vectors, popular for their graph representation and subsequent intuitive representation of causal relations. In 2018, Gissibl and Klüppelberg [11] introduced *max-linear Bayesian networks* (MLBN) to describe the causal relations of variables where large values propagate through the network. They have already been successfully applied to modeling how flooding events propagate through river networks [3, 19] and also to study tail dependencies in data from the European stock market [7].

Max-linear Bayesian networks are random vectors $X = (X_1, \dots, X_d)$ specified by a DAG $G = ([d], E)$ with weight matrix $C \in \mathbb{R}_{\geq 0}^{d \times d}$ and independent random variables Z_1, \dots, Z_d called *innovations*. An MLBN satisfies the following recursive *structural equations*

$$X_i = \bigvee_{j=1}^n c_{ij} X_j \vee Z_i \quad (1)$$

over the max-times semiring where \vee denotes taking the maximum of the operands.

Of great importance for the application of MLBNs to real-world problems is the question of inferring the structure and parameters from sample data. Previous work by Gissibl, Klüppelberg, and Lauritzen [12] has shown that an MLBN to be generally unidentifiable while characterizing the class of edge weights that could be recovered from a given sample and giving an estimator for a distinguished element of this class. Subsequently, the focus has then been on estimation of

2020 *Mathematics Subject Classification.* 05C12, 14T90, 52B11, 62R01.

Key words and phrases. max-linear Bayesian network, minimum sample size, polytrope, minimum set cover.

the edge weights for an MLBN under various assumptions, e. g. assuming regularly varying distribution tails for the innovations [16], or estimation using noisy measurements through scoring [5, 19] or Gaussian mixtures [1].

Being defined over the max-times semiring, there is a rich connection between MLBNs and tropical geometry which has been outlined by Tran [18] and that has been recently investigated by the author [2]. Using this connection, we describe the geometrical meaning of the minimum-ratio estimator proposed by Gissibl, Klüppelberg, and Lauritzen [12] and describe combinatorial properties of it. This gives rise to the question of set covers of certain subdivisions of subpolytopes of A_d root polytopes which is a combinatorial problem that can be studied in its own right.

We also combine this estimator with techniques from Buck and Klüppelberg [5] and Tran, Buck, and Klüppelberg [19] to approach the problem of structural inference for MLBNs. In addition, we conduct several computational experiments for which we make the data available under <https://zenodo.org/records/17054748>.

Outline. Section 2 contains a summary of tropical convexity and polytopes, their combinatorial properties and connection to regular subdivisions of certain point configurations and basic properties of max-linear Bayesian networks. In Section 3 we consider the minimum-ratio estimator from Gissibl, Klüppelberg, and Lauritzen [12] after applying a logarithmic transformation and describe the tropical geometric interpretation as minimum bounding polytrope of a given sample. In Section 4 we describe the properties of minimal best-case samples for which the minimum bounding polytrope can correctly identify the weight matrix when the underlying DAG is known and make a connection to minimum set covers of certain triangulations. In Section 5 we then move towards the setting where the underlying DAG is unknown and combine the minimum bounding polytrope with scoring and thresholding methods to give an algorithm for structural inference. In Section 6 we apply our method to simulated and real-world data and discuss its performance. We conclude with an outlook on the question of minimal set covers for the central triangulations of root polytopes.

2. PRELIMINARIES

2.1. Tropical convexity. Denote by $\mathbb{T} := (\mathbb{R} \cup \{\infty\}, \oplus = \min, \odot = +)$ the *tropical (min-plus) semiring* where $\oplus = \min$ and $\odot = +$. We define the *tropical affine space* \mathbb{TA}^{d-1} as the set of points $x \in \mathbb{R}^d$ with the equivalence relation given by (tropically) scaling, that is

$$(x_1, \dots, x_n) \sim \lambda \odot (x_1, \dots, x_d) = (x_1 + \lambda, \dots, x_d + \lambda)$$

for all $\lambda \in \mathbb{R}$. Then, the *tropical projective space* \mathbb{TP}^{d-1} is defined as

$$\mathbb{TP}^{d-1} := \left(\mathbb{T}^d \setminus \{(\infty, \dots, \infty)\} \right) /_{\mathbb{R}\mathbf{1}}$$

where $\mathbf{1} = (1, \dots, 1)$. This is the compactification of \mathbb{TA}^{d-1} in the sense that the pair $(\mathbb{TP}^{d-1}, \mathbb{TA}^{d-1})$ is homeomorphic to the standard d -simplex and its interior.

Fix a finite set of n points $C \subset \mathbb{TP}^{d-1}$. By abuse of notation, we write C for this set and the $d \times n$ -matrix over \mathbb{T} whose columns are the points $c^{(i)} \in C$. Additionally, we require that no row sum of C is equal to ∞ .

The *tropical polytope* $\text{tconv}(C)$ spanned by C is then defined as the set of \mathbb{R} -linear combinations of the points in C , or equivalently, as the image of the map $\mathbb{TA}^{n-1} \rightarrow \mathbb{TA}^{d-1}$ given by left multiplication with C . Tropical polytopes are *tropically convex* in the sense that for any two points $p, q \in P$ in a tropical polytope $P \subseteq \mathbb{TA}^{d-1}$, the *tropical line segment* $\text{tconv}(\{p, q\})$ is entirely contained inside P .

The tropical projective torus \mathbb{TA}^{d-1} may be identified with Euclidean space \mathbb{R}^{d-1} normalizing a coordinate to 0. Since the equivalence relation on \mathbb{TA}^{d-1} allows us to scale the coordinates of a point freely and for any representative of $p \in \mathbb{TA}^{d-1}$ all coordinates are finite, this is possible for every coordinate. A common choice is to normalize the first coordinate, that is

$$p = (p_1, p_2, \dots, p_d) \equiv (0, p_2 - p_1, \dots, p_d - p_1)$$

where $p_2 - p_1, \dots, p_d - p_1$ constitute the coordinates of p in \mathbb{R}^{d-1} .

Under the identification of \mathbb{TA}^{d-1} with \mathbb{R}^{d-1} we may compare tropical convexity with classically convexity, but it turns out that these notions are not equivalent. A tropical polytope is in general a polyhedral complex. In the special case where a tropical polytope P is classically convex, we say that P is a *polytrope* going back to Joswig and Kulas [14].

Among tropical polytopes, polytropes enjoy many special properties that simplify computations. For one, polytropes are tropical simplices, that is, for a polytrope $P \subset \mathbb{TA}^{d-1}$ we can find a square matrix $C \in \mathbb{T}^{d \times d}$ such that $P = \text{tconv}(C)$. Additionally, polytropes are polyhedra in the classical sense which means they carry a facet description given by classical linear inequalities. In particular, this facet description can be obtained as

$$Q(C) := \{x \in \mathbb{TA}^{d-1} \mid x_i - x_j \leq c_{ij} \text{ where } 1 \leq i \neq j \leq d\}.$$

The construction of $Q(C)$ is known as *weighted digraph polyhedron*.

Our exposition suggests that there is a single tropical square matrix $C \in \mathbb{T}^{d \times d}$ that realizes a given polytrope P as tropical convex hull $\text{tconv}(C)$ and as weighted digraph polyhedron $Q(C)$. To make this connection precise, recall that the *Kleene star* C^* of a tropical square matrix C is given by the power series

$$C^* := I^m \oplus C \oplus C^2 \oplus \dots \oplus C^{d-1} \oplus \dots$$

where all operations are taken over the tropical semiring.

Basic properties of the Kleene star are that multiplication by C^* is idempotent, $c_{ii}^* = 0$ and that the entries satisfy the triangle inequality

$$c_{ij}^* \leq c_{ik}^* + c_{kj}^*. \quad (2)$$

Also, taking the Kleene star of a matrix C preserves weighted digraph polyhedra, that is $Q(C) = Q(C^*)$.

Lemma 2.1 ([13, Lemma 3.24.]). *For any $C \in \mathbb{T}^{d \times d}$, if C^* converges, then $Q(C) = Q(C^*)$.*

In addition, the inequalities of $Q(C^*)$ are tight while some inequalities might be redundant. In total, we can say that for a polytrope $P \subseteq \mathbb{TA}^{d-1}$ there exists a tropical square matrix $C \in \mathbb{T}^{d \times d}$ such that

$$P = \text{tconv}(C^*) = Q(C^*) = Q(C). \quad (3)$$

In particular, C^* gives a tropical vertex and a classical facet description of P .

2.2. Max-linear Bayesian models and data generation. We turn to max-linear Bayesian networks which are a *recursive structural equation model* defined over the max-times semiring and have been introduced by Gissibl and Klüppelberg [11].

Definition 2.2. For a weighted DAG $G = (V, E)$ with weight matrix $C \in \mathbb{R}_{\geq 0}^{d \times d}$ define the *max-linear Bayesian network* (MLBN) $X = (X_1, \dots, X_n)$ by the equations

$$X_i = \bigvee_{j=1}^d c_{ij} X_j \vee c_{ii} Z_i, \quad i = 1, \dots, n, \quad (4)$$

where $Z = (Z_1, \dots, Z_n)$ are assumed to be independent random variables, each with support $\mathbb{R}_{>0}$ and atom-free distributions.

We may write above recursive linear system of equations compactly as the max-times matrix-vector product

$$X = C \cdot X \vee Z.$$

By repeated substitution, this recursive equation system admits the solution

$$X = C^* \cdot Z \quad (5)$$

where C^* is the Kleene star over the max-times semiring. By assumption, C is the weight matrix of a directed acyclic graph making C^* always well-defined.

After applying a logarithmic transformation, the set of possible observations for X forms a polytrope in \mathbb{TA}^{d-1} due to (3) and (5). This has two implications for MLBNs. For one, there is a correspondence between the weights of the underlying DAG of an MLBN and the facets of $Q(-\log C)$. On the other hand, to generate data for simulations as in Section 6.1, it suffices to generate data for the innovations Z_i and (tropically) multiply those with the Kleene star of a weight matrix C .

To make use of the identification of \mathbb{TA}^{d-1} with Euclidean space, we will implicitly apply a negative logarithmic transformation in the remainder of this work and consider MLBNs over the min-plus semiring.

2.3. Regular subdivisions of root polytopes. To study the combinatorial properties of polytopes, we define a certain point configuration as a combinatorial dual. This has been subject in [2, 15] and we recall the necessary details in the following.

Definition 2.3. For a digraph G define the associated *root polytope* as

$$P_G = \text{conv}(\{0\} \cup \{e_{ij} := e_i - e_j \mid j \rightarrow i \in G\}) \subset \mathbb{R}^d.$$

A polyhedral subdivision of a polytope $P = \text{conv}(V)$ in \mathbb{R}^d is called *regular* if it is induced by a height function $h \in \mathbb{R}^V$. For further details, see [13, Section A.4.]. We say that a subdivision Σ of P_G is *central* if the vertex 0 is contained in every cell of Σ .

Central subdivisions of root polytopes play an important role in the combinatorial characterization of polytopes due to the following result that has been shown first by Joswig and Schröter [15] for the case of the complete graph $G = K_d$ and later by Améndola and Ferry [2] for arbitrary directed graphs.

Theorem 2.4 ([2, Thm. 3.9]). *The combinatorial types of full-dimensional polytropes in \mathbb{TA}^{d-1} are in bijection with the regular central subdivisions of P_G where G ranges over transitive directed graphs G on d nodes.*

Since all subdivisions of interest are central and the origin is not an interior point of P_G whenever G is acyclic, we may perform a small reduction step that allows us to reduce the dimensionality of the objects handled. In particular, for a central subdivision Σ of P_G , we may see every cell $\sigma \in \Sigma$ as a pyramid over a polytope only involving $e_i - e_j$ vertices.

Thus, to any subdivision Σ of P_G we can associate a subdivision Σ' of the vertices of P_G excluding the origin 0 by taking for each cell $\sigma \in \Sigma$ the unique facet not containing the origin. This is called the *link* of the origin in Σ . An example of this is shown in Figure 1.

We say that a MLBN supported on a DAG G is *generic* if the weight matrix C induces a central triangulation of P_G . The subdivision of P_G induced in this way is called the *dual subdivision* to $Q(C)$.

This correspondence has a consequence on the number of pseudoverties of a polytrope. This is stated in the following well-known result that has been noted by Develin and Sturmfels [6] for tropical polytopes but ultimately goes back to work of Gelfand, Graev, and Postnikov [10]. We include a short summary of the proof.

Lemma 2.5. *If $C \in \mathbb{T}^{d \times d}$ is a lower-triangular matrix and $Q(C)$ is full-dimensional, the number of pseudoverties of $Q(C)$ is at most the $(d - 1)$ -st Catalan number*

$$C_{d-1} = \frac{1}{d} \binom{2(d-1)}{d-1}.$$

Proof. A polytrope $Q(C)$ for lower-triangular C is dual to a subdivision of a subpolytope of P_{κ_d} . The root polytope P_{κ_d} itself has been studied by Gelfand, Graev, and Postnikov and has been found to have normalized volume equal to the $(d - 1)$ -st Catalan number C_{d-1} [10, Theorem 2.3]. In particular, a triangulation of P_{κ_d} has C_{d-1} many simplices and $Q(C)$ has as many pseudoverties. \square

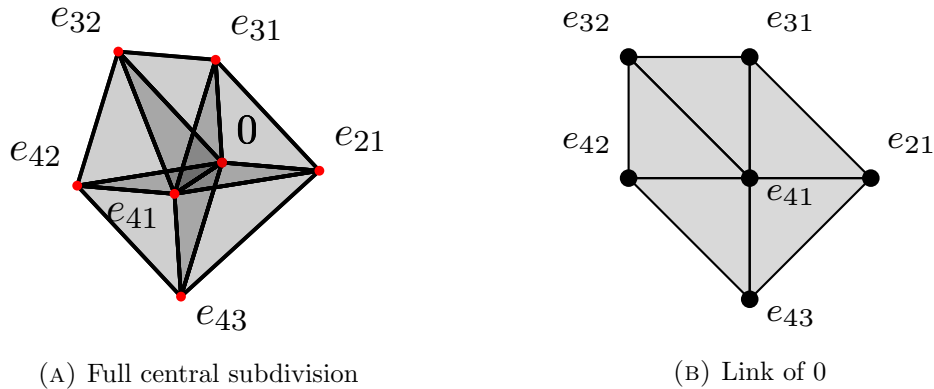


FIGURE (1). A central triangulation Σ of the root polytope P_{κ_4} and the link of the origin in Σ .

3. CALCULATING MINIMUM BOUNDING POLYTOPES

The goal of this section is to calculate a *minimum bounding polytrope* $P(S) \subset \mathbb{TA}^{d-1}$ efficiently given a finite set of points $S = \{p^{(1)}, \dots, p^{(n)}\} \subset \mathbb{TA}^{d-1}$. We can simplify this problem by making use of the classical facet description of a polytrope given by inequalities

$$x_i - x_j \leq c_{ij} \quad (6)$$

for a matrix $C \in \mathbb{T}^{d \times d}$ with $c_{ii} = 0$.

We obtain a matrix $\tilde{C} \in \mathbb{T}^{d \times d}$ by taking all maxima over S of the coordinate differences,

$$\tilde{c}_{ij} := \max_k p_i^{(k)} - p_j^{(k)}. \quad (7)$$

Proposition 3.1. *Let $S \subset \mathbb{TA}^{d-1}$ be a set of n points. Then, the matrix \tilde{C} provides a facet description of $P(S)$ and the inequalities are tight. In particular, $\tilde{C}^* = \tilde{C}$.*

Proof. The first part is by construction. To see that $\tilde{C}^* = \tilde{C}$, assume to the contrary. Then, there is an entry $\tilde{c}_{ij}^* \leq \tilde{c}_{ij}$. There also exists a point $p^{(k)}$ such that $\tilde{c}_{ij} = p_i^{(k)} - p_j^{(j)}$. But then, $p^{(k)} \in Q(\tilde{C})$ and $p^{(k)} \notin Q(\tilde{C}^*)$, which means $Q(\tilde{C}) \neq Q(\tilde{C}^*)$, contradicting Theorem 2.1. \square

This also shows that $P(S)$ is a smallest polytrope with the property that $S \subset P(S)$, and \tilde{C} constitutes a tropical vertex description of $P(S)$, which means $P(S) = \text{tconv}(\tilde{C})$.

We also get an upper bound on the calculation of the minimum bounding polytrope from Theorem 3.1. This has been observed before by Tran, Buck, and Klüppelberg [19, Lem. S2] in the context of estimating MLBNs on trees and by Miné [17] in the context of static program analysis with loops over domains that can be represented by polytopes.

Proposition 3.2. *For a finite set $S \subset \mathbb{TA}^{d-1}$ of n points, the minimum bounding polytrope $P(S)$ can be calculated using $\mathcal{O}(d^2n)$ -many comparison operations.*

In the next step, we now assume that $S \subset Q(C)$ for some matrix $C \in \mathbb{T}^{d \times d}$. For this, we have the following expected containment.

Lemma 3.3. *Let $S \subset Q(C)$ be a set of n points. Then, $P(S) \subset Q(C)$.*

Proof. It follows from (6) that for every $p \in S$ the inequalities

$$p_i - p_j \leq c_{ij}$$

are satisfied for all $i \neq j \in [d]$. But this also gives the bound

$$\tilde{c}_{ij} = \max_k p_i^{(k)} - p_j^{(k)} \leq c_{ij}.$$

Applying (6) to $P(S)$ implies that every point $p \in P(S)$ satisfies

$$p_i - p_j \leq \tilde{c}_{ij} \leq c_{ij}$$

which means that $P(S) \subset Q(C)$. \square

Since the weight c_{ij} might not define a facet of $Q(C)$, and for specific $S \subset Q(C)$ we might have $\tilde{c}_{ij} \leq c_{ij}$, $P(S)$ might exhibit more facets than $Q(C)$.

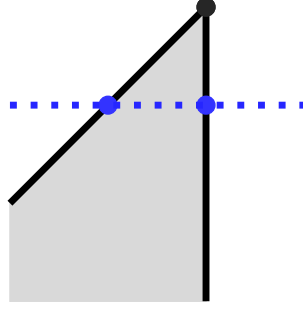


FIGURE (2). A schematic of Theorem 3.4 where $P(S)$ exhibits more facets than $Q(C)$. The additional facet of $P(S)$ is given by the dotted blue line.

Example 3.4. Suppose $G = \kappa_3$ and $C \in \mathbb{T}^{3 \times 3}$ such that $c_{31} \geq c_{32} + c_{21}$. In this case, the $x_3 - x_1$ -hyperplane does not define a facet of $Q(C)$. If in a sample S we observe that $\tilde{c}_{31} < c_{31}^*$, then in particular $P(S)$ will have a facet supported by a $x_3 - x_1$ -hyperplane. This is shown in Figure 2.

4. PARAMETER RECOVERY AND SET COVERS

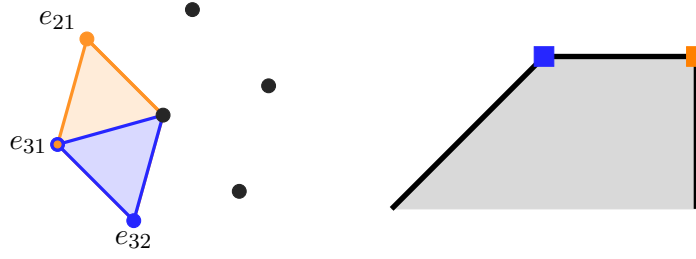
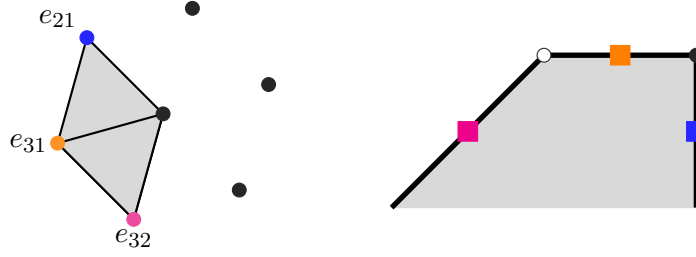
In this section, we discuss estimating the *true weight matrix* C of the MLBN using the minimum bounding polytrope in the setting where the underlying DAG G is known. Since a sample S is necessarily bounded, the maxima of every difference $X_{ij} := X_i - X_j$ will be finite and \tilde{C} will be supported on the complete graph K_d . Thus, estimating C from \tilde{C} includes selecting a subset of the entries that give a matrix $\hat{C} \in \mathbb{T}^{d \times d}$ that is supported on a DAG. In the current setting where the underlying DAG G is known, we set

$$\hat{C} := \tilde{C}|_G \quad \text{where} \quad \hat{c}_{ij} := \begin{cases} \tilde{c}_{ij}, & \text{if } j \rightarrow i \in G, \\ \infty, & \text{otherwise.} \end{cases}$$

Note that since $Q(C) = Q(C^*)$, we also have $c_{ij}^* \leq c_{ij}$. Depending on the true weights, this makes it impossible to recover certain c_{ij} , since we can at most expect to recover the entries of C^* . The extent to which the parameters of an MLBN can be identified has been studied by Gissibl, Klüppelberg, and Lauritzen [12] while Améndola and Ferry [2] gave a polyhedral description of the parameter matrices that could be observed for fixed true parameter matrix. For this reason, we assume that $C^* = C$ and that we are trying to estimate this Kleene star.

Note that the obtained matrix \hat{C} is not necessarily a Kleene star which necessarily happens when the known DAG G is not transitive. Since Gissibl, Klüppelberg, and Lauritzen specifically estimate the Kleene star of C , they additionally took the Kleene star of their estimate. Yet we decide to focus on the simpler estimator \hat{C} without additionally taking the Kleene star of \hat{C} . Since in the case where G is known, we are only interested in the edge weights of G and not in the redundant information provided by the Kleene star.

In addition, Gissibl, Klüppelberg, and Lauritzen [12] showed that the distribution of the difference X_{ij} contains atoms, one of which precisely occurs at c_{ij} . As a result, there is a positive probability that there is a sample point $X^{(k)} \in S$ for which $X_{ij}^{(k)} = c_{ij}$.

(A) Sample S_1 given by pseudovertices.(B) Sample S_2 given by points on the relative interior of the facets.FIGURE (3). Two examples of $\tilde{\Sigma}$ for samples from $Q(C)$ in Theorem 4.1.

For these reasons, in any sample $S \subset Q(C)$ only the presence of special points is necessary for \hat{C} to recover the correct parameters. A natural question to ask is how many of these special points are necessary in the best case to recover C from \hat{C} .

For this, let Σ be the link of the origin of the regular subdivision of P_G dual to $Q(C)$ and define the following map from $Q(C)$ to Σ : associate to each point $p \in Q(C)$ the cell

$$\{e_{ji} \mid p_i - p_j = c_{ij}\}$$

of the subdivision of P_G . Then, denote by $\tilde{\Sigma}(S)$ the set of cells for each $p \in S$. The question whether $\tilde{C} = C$ for a given sample $S \subset Q(C)$ is then equivalent to asking whether for every point $e_{ji} \in P_G$ there is a $\sigma \in \tilde{\Sigma}(S)$ containing that point. That is, we ask for $\tilde{\Sigma}(S)$ to be a set cover for the subdivision Σ . We demonstrate this with the following example.

Example 4.1. Consider the MLBN given by the weight matrix

$$C = \begin{pmatrix} 0 & \infty & \infty \\ 1 & 0 & \infty \\ 2 & 3 & 0 \end{pmatrix}$$

and take the two samples

$$S_1 = \{(0, -1, 2), (0, 1, 1)\}$$

$$S_2 = \{(0, 0, 2), (0, 1, 1), (0, 0, 1)\}.$$

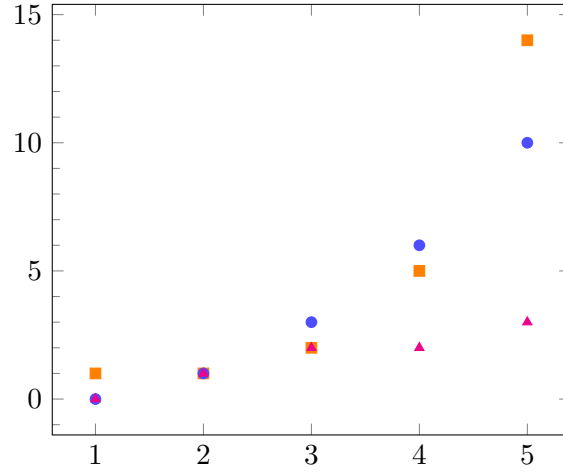


FIGURE (4). The maximal number of facets (blue circles) and pseudoverties (orange squares) of a polytrope $Q(C) \subset \mathbb{TA}^{d-1}$ when C is supported on a DAG. Also shown is the minimal best case sample size (magenta triangles) when C is supported on κ_n (compare with Table 1).

The sets $\tilde{\Sigma}$ for both samples are shown in Figure 3; they are

$$\begin{aligned}\tilde{\Sigma}(S_1) &= \{ \{e_{12}\}, \{e_{13}, e_{23}\} \}, \text{ and} \\ \tilde{\Sigma}(S_2) &= \{ \{e_{13}\}, \{e_{23}\}, \{e_{12}\} \}.\end{aligned}$$

It can be seen in Figure 3 that S_1 covers every facet of $Q(C)$ using two points while S_2 covers every facet in three points.

Above example also shows two natural choices for special points in samples for recovering C from \hat{C} which correspond to two trivial set covers of Σ .

If a sample S contains a point in each facet as in Figure 3b, $\tilde{\Sigma}(S)$ certainly covers the vertices of Σ . This leaves us with a sample of size at most $\frac{(d-1)(d-2)}{2}$, since this is the maximal number of facets for $Q(C)$ when C is supported on a DAG.

On the other hand, if $\tilde{\Sigma}(S)$ is the set of all maximal dimensional cells of Σ we also get a set cover. In this case, S has to contain all the pseudoverties of $Q(C)$ of which there are as many as the $(d-1)$ -st Catalan number C_{d-1} by Theorem 2.5.

Figure 4 shows a comparison of the maximal number of facets with the maximal number of pseudoverties for a $d-1$ -dimensional polytrope. It turns out that both options for a sample do not constitute a minimal set of special points to recover C from \hat{C} , as the following example shows.

Example 4.2. Let $G = \kappa_4$ and suppose that C is generic. There are two possible cases for the combinatorial structure of $Q(C)$ corresponding to the two central regular triangulations of P_G , which are shown in Figure 5.

In both cases, $Q(C)$ has six facets and five pseudoverties, which can be read off Figure 4 for $d=4$ but can also be seen from Figure 5 since P_G has six vertices (apart from the origin) and both triangulations have five maximal cells.

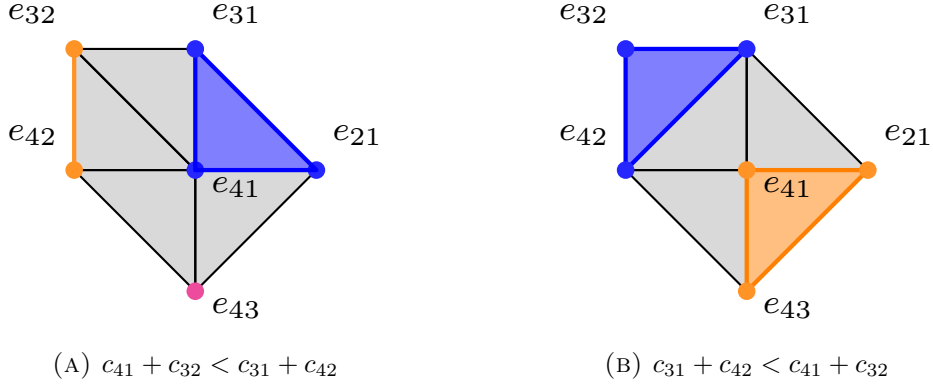


FIGURE (5). Two central regular triangulations of P_{κ_4} from Theorem 4.2 with a minimal set cover.

Yet for both triangulations the vertex cover given by all maximal cells is not a minimal set cover, and a minimal set cover is shown in Figure 5. One can also see that the minimal size depends on the subdivision and not just the subdivided point configuration.

This example also shows that the minimum sample size for the estimator \tilde{C} depends on the combinatorial type of C . Thus, for a subdivision of P_G denote by $c(\Sigma)$ the size of a minimum set cover of Σ . In analogy to set covers for graphs we call this the *set cover number* of Σ . Then, we define the *minimum sample size* $c(G)$ for MLBNs supported on G as the maximum of the set cover numbers for triangulations of P_G ,

$$c(G) := \max\{c(\Sigma) \mid \Sigma \text{ is a regular central subdivision of } P_G\}.$$

For our computations, we solely considered regular central triangulations of P_{κ_d} . This is the maximal case as both the set cover number of a subdivision and the minimum sample size exhibit a certain monotonicity in the following sense.

Lemma 4.3. *Let $C \in \mathbb{T}^{d \times d}$ be supported on G and Σ be the regular subdivision of P_G induced by C . If Σ' is a subdivision of P_G refining Σ , then $c(\Sigma) \leq c(\Sigma')$.*

Proof. Suppose $\tilde{\Sigma}'$ is a minimal set cover for Σ' . From this, we get a set cover $\tilde{\Sigma}$ for Σ by replacing every cell $\sigma' \in \tilde{\Sigma}'$ by the cell $\sigma \in \Sigma$ which is refined by σ' . Then, this set cover $\tilde{\Sigma}$ is not necessarily minimal, which gives $c(\Sigma) \leq c(\Sigma')$. \square

Remark 4.4. We can see from Theorem 4.2 that the bound provided by Theorem 4.3 is not tight in general. Denote by Σ_A and Σ_B the two central regular triangulations of P_{κ_4} that are shown in Figure 5 and let Σ' be the common coarsening of Σ_A and Σ_B . This is the subdivision without a diagonal in the upper left square (see Figure 6).

The set cover of Σ_A from Figure 5a translates directly to a set cover of Σ' which means that $c(\Sigma') \leq 3$. But following the proof of Theorem 4.3, the set cover of Σ_B translates to a set cover of Σ' by replacing

$$\sigma' = \{e_{13}, e_{23}, e_{24}\} \text{ with } \sigma = \{e_{13}, e_{14}, e_{23}, e_{24}\}.$$

This gives the upper bound $c(\Sigma') \leq 2$ which turns out to be sharp in this case.

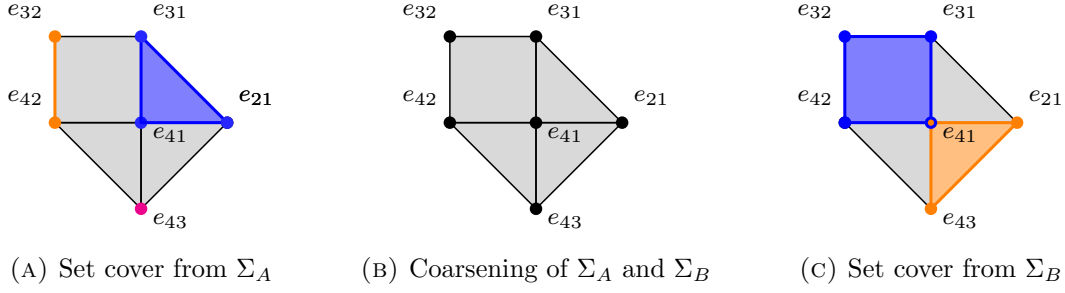


FIGURE (6). Coarse subdivision from Theorem 4.4 together with set covers obtained from the triangulations from Theorem 4.2 by applying Theorem 4.3.

Lemma 4.5. *Let $H \subseteq G$ be DAGs. Then, $c(H) \leq c(G)$.*

Proof. Let Σ' be a central regular triangulation of P_H realizing the minimum sample size for H , meaning $c(\Sigma') = c(H)$. Assume first that H is equal to G with an edge $j \rightarrow i$ removed.

We can extend Σ' into a subdivision Σ for P_G by replacing every cell $\sigma' \in \Sigma'$ visible from e_{ji} with $\sigma = \text{conv}(\sigma' \cup \{e_{ji}\})$. By visible we mean that the line segment connecting e_{ji} with the barycenter of σ' intersects Σ' only in σ' , see Figure 7. In particular, a minimum set cover for Σ' stays a minimum set cover for Σ by replacing any σ' as above with σ .

This subdivision Σ is not a triangulation of P_G , but still central and regular and as such is refined by a central regular triangulation Σ'' of P_G . Theorem 4.3 implies that $c(\Sigma) \leq c(\Sigma'')$. Summarizing the above, we get

$$c(H) = c(\Sigma') = c(\Sigma) \leq c(\Sigma'') \leq c(G).$$

We can now generalize this to arbitrary pairs $H \subseteq G$ by using the above argument inductively for each edge in $G \setminus H$. \square

For moderate d we have computationally investigated the minimum set covers of triangulations for P_{κ_d} . We employed a simple randomized greedy algorithm (Algorithm 1) with 100 repetitions to calculate a set cover for each triangulation. For each triangulation this yields a minimal observed cardinality of a set cover and for each d the observed minima are shown in Table 1.

For $d \leq 7$ we were able to iterate through all triangulations of P_{κ_d} , while for $d \geq 8$ we decided to sample a 5000 triangulations and find the size of minimal set covers with above randomized procedure.

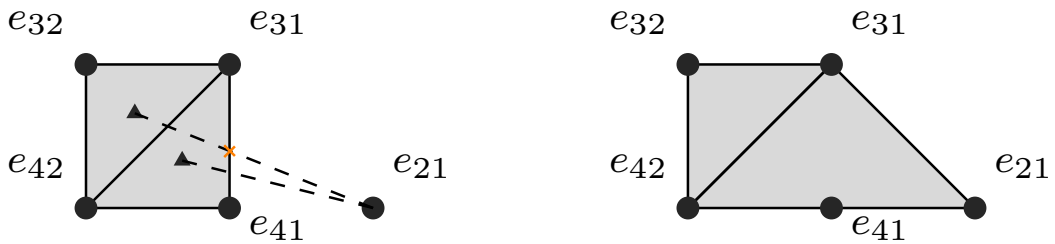


FIGURE (7). Extending a subdivision Σ' for P_H to a subdivision Σ for P_G by extending the cells visible from a new point e_{ji} .

TABLE (1). Observed set cover numbers across combinatorial types of $Q(C)$ for generic $C \in \mathbb{T}^{d \times d}$ supported on $G = \kappa_d$. For $(*)$, the observed set cover numbers are obtained from a sample of 5000 triangulations.

d	1	2	3	4	5	6	7	$8^{(*)}$	$9^{(*)}$
	0	1	2	2,3	3	3,4	4,5	5,6	5,6,7

Algorithm 1 Randomized greedy set cover for triangulations

Input: triangulation Σ for a point configuration P

- 1: $\tilde{\Sigma} \leftarrow \emptyset$
 - 2: **while** there exists $p \in P$ not covered by $\tilde{\Sigma}$ **do**
 - 3: Choose $\sigma \in \Sigma$ with the least covered elements $p \in P$
 - 4: $\tilde{\Sigma} \leftarrow \tilde{\Sigma} \cup \{\sigma\}$
 - 5: **return** $\tilde{\Sigma}$
-

5. STRUCTURAL LEARNING AND GAPS

In the regime where we do not know the underlying DAG G but do know that the ordering of the coordinates corresponds to a topological ordering of G , we find ourselves in a slight variation of the situation where we assume $G = \kappa_d$.

In the worst case we need to estimate as many edges as in the case when $G = \kappa_d$ is actually known, but we have to estimate the existence an edge additionally. Thus, we cannot obtain an estimate \hat{C} by simply calculating \tilde{C} and restricting to entries corresponding to known edges.

A simple condition to check whether the maximum of X_{ij} corresponds to an atom, and thus an edge, is to check whether $X_{ij} = \tilde{c}_{ij}$ multiple times in a given sample [12]. Alternatively, there are more involved scoring methods based on concentration measures for X_{ij} that have been shown by Tran, Buck, and Klüppelberg [19] to work in the case of MLBNs with underlying DAG being a tree.

To *score* whether an observed maximum of X_{ij} corresponds to an edge, we want a non-negative function s that given the observations for X_{ij} produces a small number if there is a high concentration around the maximum of X_{ij} , indicating an atom and thus the presence of an edge. The following are some possible choices for *scoring functions*:

- The *top- k gap* that compares the maximum of X_{ij} with the k -th highest observation (assuming that the observations of X_{ij} are sorted from largest to smallest),

$$s_{ij}(k) := \left(X_{ij}^{(1)} - X_{ij}^{(k)} \right)^2.$$

- The empirical *quantile-to-mean gap* that compares an upper quantile with the mean,

$$s_{ij}(\bar{r}) := \frac{(\mathbb{E}[X_{ij}] - Q_{X_{ij}}(\bar{r}))^2}{n_{ij}}.$$

- The empirical *upper quantile gap* that compares two fixed quantile levels,

$$s_{ij}(\bar{r}, \underline{r}) := \frac{(Q_{X_{ij}}(\bar{r}) - Q_{X_{ij}}(\underline{r}))^2}{n_{ij}}.$$

If we additionally assume that the ordering of the coordinates is not necessarily known, we additionally have to decide whether the maximum of X_{ij} or the maximum of X_{ji} (which is the minimum of X_{ij}) exhibits an atom and which one scores better. For this, we combine the scoring approach from Tran, Buck, and Klüppelberg with thresholding proposed by Buck and Klüppelberg [5]. These considerations are put together in Algorithm 2 to calculate an estimate \hat{C} given a sample S from a MLBN by calculating \tilde{C} for the minimum bounding polytrope of S and pruning edges.

Algorithm 2 Estimating \hat{C} for a MLBN with unknown DAG and ordering

Input: Sample $S := \{p^{(1)}, \dots, p^{(n)}\}$ originating from an MLBN

Parameter: threshold $t > 0$, a scoring function s

```

1:  $\hat{C} \leftarrow \left( \max_k p_i^{(k)} - p_j^{(k)} \right)_{1 \leq i, j \leq d}$  ▷ minimum bounding polytrope for  $S$ 
2: Compute the scores  $s_{ij}$ 
3: for  $1 \leq i \neq j \leq d$  do
4:   if  $s_{ij}, s_{ji} \geq t$  then
5:      $\hat{c}_{ij}, \hat{c}_{ji} \leftarrow \infty$  ▷ Neither direction between  $i$  and  $j$  is present
6:   else if  $s_{ij} < s_{ji}$  then
7:      $\hat{c}_{ji} \leftarrow \infty$  ▷  $j \rightarrow i$  is present
8:   else
9:      $\hat{c}_{ij} \leftarrow \infty$  ▷  $i \rightarrow j$  is present
10: return  $\hat{C}$ 

```

6. EXPERIMENTS ON DATA

We test Algorithm 2 in several settings, on simulated data and on two real-world datasets. The code to reproduce our experiments is available under the following link:

<https://zenodo.org/records/17054748>

To estimate the performance of our method, we use standard performance metrics in causal inference [20] that have also been used in [19] for the evaluation of the methods therein. We recall the definitions of those in the following.

Denote by $\text{SHD}(G, \hat{G})$ the *structural Hamming distance* between G and the estimate \hat{G} , which is the minimal number of edge additions, deletions and reversals necessary to turn \hat{G} into G . Denote by E and \hat{E} the set of edges of G respectively \hat{G} . Then, $E \cap \hat{E}$ is the set of correctly estimated edges while $\hat{E} \setminus E$ contains the edges that have been estimated incorrectly, either by reversal of direction or not being present in G . Applying appropriate normalizing factors, we obtain the following four quantities:

$$\begin{aligned}
 \text{nSHD}(G, \tilde{G}) &:= \frac{\text{SHD}(G, \tilde{G})}{\#E + \#\tilde{E}}, & \text{FDR}(G, \tilde{G}) &:= \frac{\#(\tilde{E} \setminus E)}{\#\tilde{E}}, \\
 \text{FPR}(G, \tilde{G}) &:= \frac{\#(\tilde{E} \setminus E)}{d(d-1) - \#E}, & \text{TPR}(G, \tilde{G}) &:= \frac{\#(E \cap \tilde{E})}{\#E}.
 \end{aligned}$$

The *false discovery rate* FDR describes the ratio of incorrectly estimated edges among all estimated edges, the *false positive rate* FPR describes the ratio of incorrectly estimated edges

compared to all non-present edges in G while the *true positive rate* is the ratio of correctly estimated edges.

6.1. Simulated data. For our simulation study, we have generated data S from a max-linear Bayesian network using (5) assuming $Z_i \sim D$ i.i.d. for some distribution D . For the parameter matrix C , we draw each weight c_{ij} uniformly from a fixed interval $[-\tau, \tau]$ for some $\tau \geq 0$ and select each edge $j \rightarrow i \in G$ with fixed probability $p \in (0, 1]$. This way, we obtain a lower-triangular matrices $C \in \mathbb{T}^{d \times d}$ as parameter matrix.

We performed simulations for both the setting of known DAG G as in Section 4 and unknown DAG with unknown ordering as in Section 5. For the latter setting, we additionally generated a permutation $\sigma \in \mathbb{S}_d$ to obtain a random ordering of the nodes of G . We simulated for graphs of sizes $d = 5, 10, 30, 50, 100$ with 5000 repetitions with sample size $N = 1000$ for each simulation. For the scoring functions, we have used the top-k gap with $k = 30$ and the quantile-to-mean gap with $\bar{r} = 0.95$.

We considered the following settings for the distributions of the innovations Z_i and selection of the model parameters:

- (1) Gaussian i.i.d. innovations and $G = \kappa_d$ ($p = 1$),
- (2) Gaussian i.i.d. innovations and $p = \frac{1}{2}$,
- (3) Fréchet i.i.d. innovations and $G = \kappa_d$ ($p = 1$), and
- (4) Fréchet i.i.d. innovations and $p = \frac{1}{2}$.

Each setting was simulated with a fixed ordering where C is lower-triangular (Table 3 and Table 5), and with a random ordering of the coordinates (Table 4 and Table 6).

Our results show that Algorithm 2 performs reasonably well for MLBNs of moderate size, that is with underlying DAGs on $d \leq 30$ nodes, when using the top-k gap as scoring function. In this case, the performance is slightly worse for Fréchet distributed innovations than for Gaussian distributed ones. Also, the algorithm with top-k gap performs similarly for instances with known ordering and for instances with random, unknown ordering.

When using the quantile-to-mean gap as scoring function, the performance of Algorithm 2 is worse than using top-k gap. For large graphs ($d = 50, 100$), the true positive rate is close to 50% indicating that this variant performs similar to randomly guessing the edges. Additionally, the performance for Fréchet distributed innovations is worse which could be due to the presence of extreme outliers. This also supports our observation that when using the quantile-to-mean gap as scoring function the threshold in Algorithm 2 has to be adjusted to the specific scenario.

6.2. Dietary supplement data. In this experiment, we consider dietary supplement data of $n = 8327$ independent interviews taken from the NHANES report for the period 2015–2016. This data has been originally available from

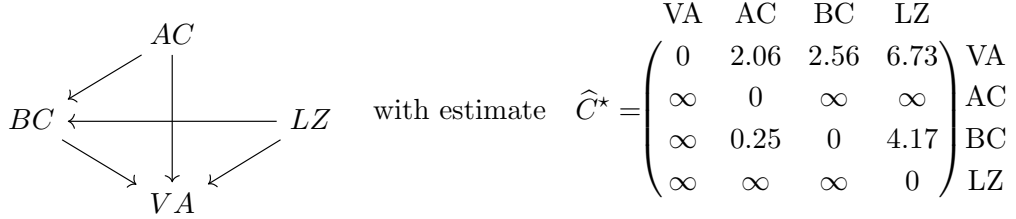
https://www.cdc.gov/Nchs/Nhanes/2015-2016/DR1TOT_I.XPT

but at the time of writing this dataset has not been available from its original address and instead had to be retrieved from the Internet Archive.

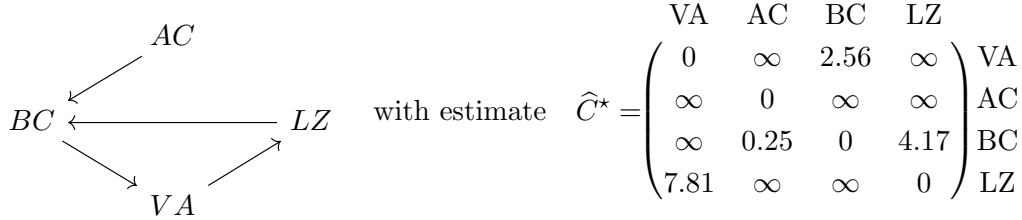
This dataset has been used in [16, 5] to test the performance of the therein developed estimators for MLBNs. In both cases the focus was on four of the 168 data components which describe the intake of Vitamin A (DR1TVARA), Beta-Carotene (DR1TBCAR), Lutein+Zeaxanthin

(DR1TLZ) and Alpha-Carotene (DR1TACAR). We abbreviate these components as VA, BC, LZ, AC respectively. For preprocessing, we only applied a negative logarithmic transformation to these four components.

For Algorithm 2 together with the top-k gap, we recovered the following DAG. We additionally give the Kleene star \hat{C}^* of our estimate for sake of comparability with [16, 5]. The DAG agrees with the one obtained by [5, Section 6.1] but is missing the edge $AC \rightarrow LZ$ of the DAG estimated by [16, Section 7.3].



When using the empirical quantile-to-mean gap as scoring function, we obtained a directed graph with a cycle. This shows an important caveat about our method since there is no guarantee that the estimated graph contains no cycles.



6.3. The upper Danube network. The Danube network data consist of daily measurements collected at $d = 31$ gauging stations in the Danube river basin over 50 years from 1960 to 2009 by the Bavarian Environmental Agency. This region is prone to serious flooding which provides the extreme events to apply MLBNS to.

This dataset has been a mainstay in benchmarking statistical methods for estimating MLBNS [8, 19]. We have used the version of this dataset included in [9] which incorporates the preprocessing by [3]. This includes restricting the data to the months June, July and August since the most extreme flooding events occur at this time due to heavy summer rain [4].

While fitting using the top-k gap and quantile-to-mean gap as scoring method, we did not recover the true graph successfully. While our method recovered some edges also present in the true network, there is also a large amount of edges in the estimated DAG either in the wrong direction or not present in the true network. The results for both attempts are given in Table 2.

Inspecting a slice (Figure 8) along the $X_2 - X_3$ and $X_1 - X_3$ coordinates reveals that while there is a visible diagonal line along which the sample concentrates which corresponds to the edge $2 \rightarrow 1$ there are sample points lying beyond this diagonal line. These points interfere with our approach since by calculating \tilde{C} we just take the maxima without accounting for noise.

7. AN OPEN QUESTION

In Section 4, we studied lower bounds on the size of special samples to completely recover the weights of an MLBN on a DAG G . We did this in terms of minimal set covers of regular

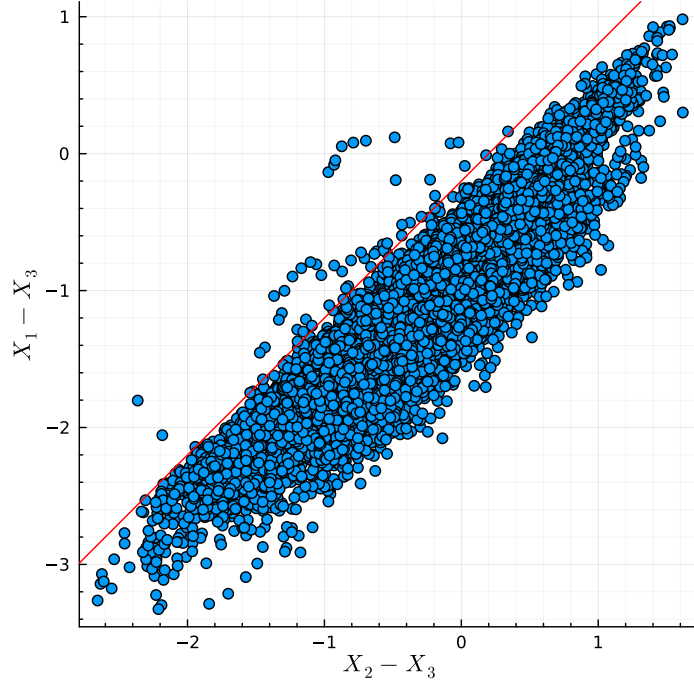


FIGURE (8). A slice of the upper Danube data plotted in the X_{32} – X_{31} -plane. The orange line shows the supposed hyperplane corresponding to the edge $2 \rightarrow 1$ that is obscured by the noise lying above.

	parameters	nSHD	FDR	FPR	TPR
top- k	$k = 203$	58.0%	64.8%	18.9%	51.9%
quantile-to-mean	$\bar{r} = 0.95$	72.3%	81.9%	52.3%	58.4%

TABLE (2). Metrics for the DAGs estimated from the upper Danube network

central subdivision of P_G and obtained the minimum sample size $c(G)$ as the maximum of those set cover numbers.

While we laid the groundwork to study those minimal set covers, there is an immediate questions that serve as next step in understanding those set covers and the minimum sample size.

Question 1. Is there an expression for the sequence $(c(\kappa_d))_{d \in \mathbb{N}}$ as recurrence relation or in closed form and does it relate to other known sequences?

For example, the entries from Table 1 for $d \leq 7$ suggest that $c(\kappa_d)$ is the maximum of two numbers, which is not supported by the evidence for $d = 9$. Also, while closely related to the well-known formula for the sum of the first $d - 1$ numbers, $c(\kappa_d)$ is not just the number of terms in this sum, that is, $c(\kappa_d) \neq d$. The difference is that compared to the sum of the first $d - 1$ numbers, a minimum set cover for a subdivision Σ gives a different expression for $\frac{(d-1)(d-2)}{2}$ via

$$\sum_{\sigma \in \Sigma} \#\sigma = \frac{(d-1)(d-2)}{2}$$

where compared to the expression as the sum of the first $d - 1$ numbers several of the simians are combined if there is an appropriate $\sigma \in \Sigma$.

On the other hand, when trying to understand the structures of the minimal set covers, note that any set cover $\tilde{\Sigma}$ corresponds to a decomposition of G as a spanning forest where the choice of spanning trees is restricted according to Σ . If we assume that Σ is a triangulation, we can even assume that the spanning trees are edge-disjoint.

ACKNOWLEDGEMENTS

The author is funded by the Deutsche Forschungsgemeinschaft (DFG, German Research Foundation) under Germany's Excellence Strategy – The Berlin Mathematics Research Center MATH+ (EXC-2046/1, project ID: 390685689), Project AA3-16.

REFERENCES

- [1] Mark Adams, Kamillo Ferry, and Ruriko Yoshida. *Inference for max-linear Bayesian networks with noise*. 2025. arXiv: 2505.00229 [stat.ML] (cit. on p. 2).
- [2] Carlos Améndola and Kamillo Ferry. “Tropical combinatorics of max-linear Bayesian networks”. In: *Journal of Symbolic Computation* 134 (2026), p. 102518. ISSN: 0747-7171. DOI: 10.1016/j.jsc.2025.102518 (cit. on pp. 2, 4, 5, 7).
- [3] Peiman Asadi, Anthony C. Davison, and Sebastian Engelke. “Extremes on river networks”. In: *The Annals of Applied Statistics* 9.4 (2015). ISSN: 1932-6157. DOI: 10.1214/15-AOAS863 (cit. on pp. 1, 15).
- [4] O. Böhm and K.-F. Wetzel. “Flood history of the Danube tributaries Lech and Isar in the Alpine foreland of Germany”. en. In: *Hydrological Sciences Journal* 51.5 (Oct. 2006), pp. 784–798. ISSN: 0262-6667, 2150-3435. DOI: 10.1623/hysj.51.5.784 (cit. on p. 15).
- [5] Johannes Buck and Claudia Klüppelberg. “Recursive max-linear models with propagating noise”. In: *Electronic Journal of Statistics* 15.2 (2021), pp. 4770–4822. ISSN: 1935-7524, 1935-7524. DOI: 10.1214/21-EJS1903 (cit. on pp. 2, 13, 14, 15).
- [6] Mike Develin and Bernd Sturmfels. “Tropical convexity”. In: *Documenta Mathematica* 9 (2004), pp. 1–27. ISSN: 1431-0635, 1431-0643. DOI: 10.4171/dm/154 (cit. on p. 5).
- [7] John H. J. Einmahl, Anna Kiriliouk, and Johan Segers. “A continuous updating weighted least squares estimator of tail dependence in high dimensions”. en. In: *Extremes* 21.2 (2018), pp. 205–233. ISSN: 1386-1999, 1572-915X. DOI: 10.1007/s10687-017-0303-7 (cit. on p. 1).
- [8] Sebastian Engelke and Adrien S. Hitz. “Graphical Models for Extremes”. In: *Journal of the Royal Statistical Society Series B: Statistical Methodology* 82.4 (2020), pp. 871–932. ISSN: 1369-7412. DOI: 10.1111/rssb.12355 (cit. on p. 15).
- [9] Sebastian Engelke, Adrien S. Hitz, Nicola Gnecco, and Manuel Hentschel. *graphicalExtremes: Statistical Methodology for Graphical Extreme Value Models*. Version: 0.3.4. Nov. 8, 2019. DOI: 10.32614/CRAN.package.graphicalExtremes. URL: <https://CRAN.R-project.org/package=graphicalExtremes> (cit. on p. 15).
- [10] Israel M. Gelfand, Mark I. Graev, and Alexander Postnikov. “Combinatorics of hypergeometric functions associated with positive roots”. In: *The Arnold-Gelfand Mathematical Seminars*. Ed. by V. I. Arnold, I. M. Gelfand, V. S. Retakh, and M. Smirnov. Boston, MA: Birkhäuser, 1997, pp. 205–221. ISBN: 978-1-4612-4122-5. DOI: 10.1007/978-1-4612-4122-5_10 (cit. on p. 5).

- [11] Nadine Gissibl and Claudia Klüppelberg. “Max-linear models on directed acyclic graphs”. In: *Bernoulli* 24.4 (2018), pp. 2693–2720. ISSN: 1350-7265. DOI: 10.3150/17-BEJ941 (cit. on pp. 1, 4).
- [12] Nadine Gissibl, Claudia Klüppelberg, and Steffen Lauritzen. “Identifiability and estimation of recursive max-linear models”. In: *Scandinavian Journal of Statistics* 48.1 (2021), pp. 188–211. ISSN: 0303-6898, 1467-9469. DOI: 10.1111/sjos.12446 (cit. on pp. 1, 2, 7, 12).
- [13] Michael Joswig. *Essentials of tropical combinatorics*. Vol. 219. Graduate Studies in Mathematics. Providence, RI: American Mathematical Society, 2021 (cit. on pp. 3, 4).
- [14] Michael Joswig and Katja Kulas. “Tropical and ordinary convexity combined”. In: *Advances in Geometry* 10.2 (Apr. 1, 2010), pp. 333–352. ISSN: 1615-7168. DOI: 10.1515/advgeom.2010.012 (cit. on p. 3).
- [15] Michael Joswig and Benjamin Schröter. *The Tropical Geometry of Shortest Paths*. 2019. arXiv: 1904.01082v2 (cit. on p. 4).
- [16] Claudia Klüppelberg and Mario Krali. “Estimating an extreme Bayesian network via scalings”. In: *Journal of Multivariate Analysis* 181 (2021), p. 104672. ISSN: 0047259X. DOI: 10.1016/j.jmva.2020.104672 (cit. on pp. 2, 14, 15).
- [17] Antoine Miné. “A New Numerical Abstract Domain Based on Difference-Bound Matrices”. In: *Programs as Data Objects*. Ed. by Olivier Danvy and Andrzej Filinski. Vol. 2053. Series Title: Lecture Notes in Computer Science. Berlin, Heidelberg: Springer Berlin Heidelberg, 2001, pp. 155–172. ISBN: 978-3-540-42068-2 978-3-540-44978-2. DOI: 10.1007/3-540-44978-7_10 (cit. on p. 6).
- [18] Ngoc M. Tran. *The tropical geometry of causal inference for extremes*. July 20, 2022. arXiv: 2207.10227[math,stat] (cit. on p. 2).
- [19] Ngoc Mai Tran, Johannes Buck, and Claudia Klüppelberg. “Estimating a directed tree for extremes”. In: *Journal of the Royal Statistical Society Series B: Statistical Methodology* 86.3 (2024), pp. 771–792. ISSN: 1369-7412, 1467-9868. DOI: 10.1093/jrsssb/qkad165 (cit. on pp. 1, 2, 6, 12, 13, 15).
- [20] Xun Zheng, Bryon Aragam, Pradeep Ravikumar, and Eric P. Xing. “DAGs with NO TEARS: continuous optimization for structure learning”. In: *Proceedings of the 32nd international conference on neural information processing systems*. NIPS’18. Montréal, Canada: Curran Associates Inc., 2018, pp. 9492–9503. DOI: 10.5555/3327546.3327618 (cit. on p. 13).

KAMILLO FERRY, TECHNICAL UNIVERSITY BERLIN, GERMANY
 Email address: ferry@math.tu-berlin.de

(A) Gaussian i. i. d. innovations and $G = \kappa_d$

d	nSHD		FDR		FPR		TPR	
5	0.0%	(0.0%)	0.0%	(0.0%)	0.0%	(0.0%)	100.0%	(0.0%)
10	0.3%	(0.2%)	0.3%	(0.2%)	0.5%	(0.4%)	99.9%	(0.3%)
30	6.5%	(3.4%)	6.5%	(3.4%)	7.5%	(3.9%)	93.4%	(3.4%)
50	12.6%	(3.7%)	12.6%	(3.7%)	13.7%	(4.0%)	87.3%	(3.7%)
100	17.4%	(2.8%)	17.4%	(2.8%)	18.1%	(2.9%)	82.5%	(2.8%)

(B) Gaussian i. i. d. innovations and edge probability $p = \frac{1}{2}$

d	nSHD		FDR		FPR		TPR	
5	0.5%	(0.2%)	0.9%	(0.3%)	1.1%	(3.7%)	100.0%	(0.0%)
10	0.9%	(0.1%)	1.9%	(2.7%)	1.7%	(2.5%)	99.9%	(0.1%)
30	4.7%	(2.4%)	6.9%	(2.7%)	6.8%	(2.7%)	97.6%	(2.4%)
50	10.5%	(4.4%)	12.3%	(4.3%)	12.3%	(4.3%)	91.4%	(4.5%)
100	18.0%	(4.6%)	19.0%	(4.5%)	19.0%	(4.5%)	83.1%	(4.7%)

(C) Fréchet i. i. d. innovations and $G = \kappa_d$

d	nSHD		FDR		FPR		TPR	
5	0.0%	(0.0%)	0.0%	(0.0%)	0.0%	(0.0%)	100.0%	(0.0%)
10	0.9%	(1.5%)	0.9%	(1.5%)	1.5%	(2.3%)	99.9%	(0.1%)
30	14.2%	(5.0%)	14.2%	(5.0%)	16.3%	(5.7%)	85.8%	(4.9%)
50	17.8%	(4.6%)	17.8%	(4.6%)	19.3%	(5.0%)	82.2%	(4.6%)
100	21.6%	(3.6%)	21.6%	(3.6%)	22.5%	(3.7%)	78.4%	(3.6%)

(D) Fréchet i. i. d. innovations and edge probability $p = \frac{1}{2}$

d	SHD		FDR		FPR		TPR	
5	0.0%	(0.0%)	0.0%	(0.0%)	0.0%	(0.0%)	100.0%	(0.0%)
10	2.3%	(1.8%)	4.4%	(3.3%)	4.4%	(3.3%)	99.9%	(0.5%)
30	14.8%	(4.9%)	17.9%	(4.8%)	18.1%	(4.9%)	88.5%	(5.1%)
50	20.5%	(6.1%)	22.5%	(6.0%)	22.7%	(6.0%)	81.7%	(6.3%)
100	23.4%	(5.2%)	24.5%	(5.1%)	24.7%	(5.2%)	77.7%	(5.3%)

TABLE (3). Simulation study for fixed topological ordering and top- k gap scoring where $k = 30$

(A) Gaussian i. i. d. innovations and $G = \kappa_d$

d	SHD		FDR		FPR		TPR	
5	0.0%	(0.0%)	0.0%	(0.0%)	0.0%	(0.0%)	100.0%	(0.0%)
10	0.0%	(0.3%)	0.0%	(0.3%)	0.1%	(0.4%)	99.9%	(0.2%)
30	9.9%	(4.6%)	9.9%	(4.6%)	11.4%	(5.3%)	90.1%	(4.6%)
50	21.2%	(4.9%)	21.2%	(4.9%)	23.0%	(5.3%)	78.8%	(4.9%)
100	33.6%	(3.7%)	33.7%	(3.7%)	35.1%	(3.9%)	66.3%	(3.7%)

(B) Gaussian i. i. d. innovations and edge probability $p = \frac{1}{2}$

d	SHD		FDR		FPR		TPR	
5	0.0%	(0.0%)	0.0%	(0.0%)	0.0%	(0.0%)	100.0%	(0.0%)
10	0.9%	(1.4%)	1.7%	(2.6%)	1.6%	(2.3%)	99.9%	(0.1%)
30	5.0%	(2.6%)	7.2%	(2.9%)	7.1%	(2.9%)	97.3%	(2.7%)
50	13.2%	(5.5%)	14.9%	(5.3%)	14.9%	(5.4%)	88.7%	(5.7%)
100	27.6%	(5.6%)	28.5%	(5.5%)	28.5%	(5.6%)	73.4%	(5.7%)

(C) Fréchet i. i. d. innovations and $G = \kappa_d$

d	SHD		FDR		FPR		TPR	
5	0.0%	(0.0%)	0.0%	(0.0%)	0.0%	(0.0%)	100.0%	(0.0%)
10	1.0%	(1.5%)	1.0%	(1.5%)	1.6%	(2.4%)	99.0%	(1.5%)
30	21.2%	(5.5%)	21.2%	(5.5%)	24.9%	(6.3%)	78.3%	(5.5%)
50	31.5%	(5.2%)	31.5%	(5.2%)	34.2%	(5.6%)	68.5%	(5.2%)
100	40.1%	(3.8%)	40.1%	(3.8%)	41.7%	(3.9%)	59.9%	(3.8%)

(D) Fréchet i. i. d. innovations and edge probability $p = \frac{1}{2}$

d	SHD		FDR		FPR		TPR	
5	0.0%	(0.0%)	0.0%	(0.0%)	0.0%	(0.0%)	100.0%	(0.0%)
10	2.3%	(1.7%)	4.4%	(3.3%)	4.4%	(3.3%)	99.9%	(0.5%)
30	17.2%	(5.5%)	20.3%	(5.3%)	20.5%	(5.5%)	86.0%	(5.8%)
50	27.6%	(6.6%)	29.5%	(6.4%)	29.8%	(6.5%)	74.4%	(6.8%)
100	37.9%	(5.5%)	38.8%	(5.4%)	39.1%	(5.5%)	63.0%	(5.5%)

TABLE (4). Simulation study for random topological ordering and top- k gap scoring where $k = 30$

(A) Gaussian i. i. d. innovations and $G = \kappa_d$

d	nSHD		FDR		FPR		TPR	
5	0.9%	(2.4%)	0.9%	(2.4%)	2.8%	(7.1%)	99.1%	(2.4%)
10	8.9%	(4.9%)	8.9%	(4.9%)	14.0%	(7.5%)	91.1%	(4.8%)
30	34.8%	(7.2%)	34.8%	(7.2%)	40.0%	(8.3%)	65.2%	(7.2%)
50	40.7%	(5.9%)	40.7%	(5.9%)	44.2%	(6.4%)	59.3%	(5.9%)
100	44.4%	(3.4%)	44.4%	(3.4%)	46.2%	(3.6%)	55.6%	(3.4%)

(B) Gaussian i. i. d. innovations and edge probability $p = \frac{1}{2}$

d	nSHD		FDR		FPR		TPR	
5	15.5%	(9.7%)	25.6%	(14.4%)	39.7%	(16.0%)	99.9%	(0.9%)
10	14.3%	(5.4%)	23.1%	(8.3%)	26.6%	(7.0%)	97.5%	(3.2%)
30	24.0%	(7.8%)	27.6%	(7.3%)	28.7%	(7.7%)	79.9%	(8.5%)
50	33.6%	(8.3%)	35.6%	(8.0%)	36.3%	(8.2%)	68.5%	(8.6%)
100	41.3%	(6.4%)	42.2%	(6.3%)	42.6%	(6.4%)	59.6%	(6.5%)

(C) Fréchet i. i. d. innovations and $G = \kappa_d$

d	nSHD		FDR		FPR		TPR	
5	11.1%	(12.6%)	10.8%	(12.6%)	32.3%	(37.8%)	88.6%	(12.9%)
10	22.3%	(10.2%)	22.1%	(10.2%)	34.5%	(16.0%)	77.6%	(10.3%)
30	39.7%	(7.4%)	39.7%	(7.4%)	45.5%	(8.5%)	60.2%	(7.4%)
50	42.6%	(5.4%)	42.5%	(5.4%)	46.1%	(5.8%)	57.4%	(5.4%)
100	44.4%	(3.0%)	44.4%	(3.0%)	46.2%	(3.1%)	55.6%	(3.0%)

(D) Fréchet i. i. d. innovations and edge probability $p = \frac{1}{2}$

d	SHD		FDR		FPR		TPR	
5	24.4%	(14.2%)	32.9%	(16.4%)	53.5%	(23.6%)	88.6%	(13.7%)
10	24.9%	(10.6%)	32.3%	(11.2%)	37.5%	(11.5%)	85.0%	(11.4%)
30	36.0%	(9.4%)	38.9%	(8.9%)	40.3%	(9.3%)	67.2%	(10.0%)
50	40.5%	(8.7%)	42.2%	(8.4%)	43.0%	(8.6%)	61.3%	(9.0%)
100	43.9%	(5.8%)	44.8%	(5.7%)	45.2%	(5.8%)	56.9%	(5.9%)

TABLE (5). Simulation study for fixed topological ordering and quantile-to-mean scoring with upper quantile level $\bar{r} = 0.95$

(A) Gaussian i. i. d. innovations and $G = \kappa_d$									
d	nSHD		FDR		FPR		TPR		
5	0.9%	(2.4%)	0.9%	(2.4%)	2.8%	(7.1%)	99.1%	(2.4%)	
10	9.1%	(4.9%)	9.1%	(4.9%)	14.3%	(7.7%)	91.1%	(4.9%)	
30	35.2%	(7.5%)	35.2%	(7.5%)	40.4%	(8.7%)	64.8%	(7.5%)	
50	41.8%	(5.9%)	41.8%	(5.9%)	45.3%	(6.4%)	58.2%	(5.9%)	
100	45.9%	(3.5%)	45.9%	(3.5%)	47.8%	(3.7%)	54.0%	(3.5%)	

(B) Gaussian i. i. d. innovations and edge probability $p = \frac{1}{2}$									
d	nSHD		FDR		FPR		TPR		
5	15.5%	(9.8%)	25.6%	(14.5%)	39.7%	(16.1%)	99.9%	(0.9%)	
10	14.2%	(5.4%)	22.9%	(8.3%)	26.4%	(7.0%)	97.5%	(3.1%)	
30	24.1%	(7.6%)	27.7%	(7.1%)	28.8%	(7.5%)	79.8%	(8.3%)	
50	34.0%	(8.4%)	36.0%	(8.1%)	36.7%	(8.4%)	68.1%	(8.8%)	
100	42.0%	(6.6%)	42.9%	(6.5%)	43.3%	(6.5%)	58.9%	(6.7%)	

(C) Fréchet i. i. d. innovations and $G = \kappa_d$									
d	nSHD		FDR		FPR		TPR		
5	11.0%	(12.5%)	10.7%	(12.5%)	31.9%	(37.4%)	88.8%	(12.7%)	
10	22.3%	(10.0%)	22.1%	(10.0%)	34.7%	(15.7%)	77.6%	(10.1%)	
30	41.3%	(7.6%)	41.3%	(7.6%)	47.3%	(8.7%)	58.6%	(7.6%)	
50	44.7%	(5.4%)	44.7%	(5.4%)	48.4%	(5.9%)	55.3%	(5.4%)	
100	47.3%	(3.1%)	47.3%	(3.1%)	49.2%	(3.2%)	52.6%	(3.1%)	

(D) Fréchet i. i. d. innovations and edge probability $p = \frac{1}{2}$									
d	SHD		FDR		FPR		TPR		
5	25.1%	(14.3%)	33.8%	(16.4%)	54.4%	(23.2%)	88.6%	(13.8%)	
10	25.0%	(10.5%)	32.5%	(11.0%)	37.8%	(11.4%)	84.9%	(11.3%)	
30	36.6%	(9.5%)	39.5%	(9.0%)	40.9%	(9.4%)	66.6%	(10.2%)	
50	41.8%	(8.7%)	43.4%	(8.5%)	44.2%	(8.6%)	60.0%	(9.1%)	
100	45.5%	(6.0%)	46.3%	(5.9%)	46.7%	(6.0%)	55.3%	(6.1%)	

TABLE (6). Simulation study for random topological ordering and quantile-to-mean scoring with upper quantile level $\bar{r} = 0.95$